

<https://helda.helsinki.fi>

Spectroscopic characterization of the complex of vinyl radical and carbon dioxide : Matrix isolation and ab initio study

Ryazantsev, Sergey V.

2017-11-14

Ryazantsev , S V , Tyurin , D A , Feldman , V I & Khriachtchev , L 2017 , ' Spectroscopic characterization of the complex of vinyl radical and carbon dioxide : Matrix isolation and ab initio study ' , Journal of Chemical Physics , vol. 147 , no. 18 , 184301 . <https://doi.org/10.1063/1.5000578>

<http://hdl.handle.net/10138/313145>

<https://doi.org/10.1063/1.5000578>

publishedVersion

Downloaded from Helda, University of Helsinki institutional repository.

This is an electronic reprint of the original article.

This reprint may differ from the original in pagination and typographic detail.

Please cite the original version.

Spectroscopic characterization of the complex of vinyl radical and carbon dioxide: Matrix isolation and *ab initio* study

Cite as: J. Chem. Phys. **147**, 184301 (2017); <https://doi.org/10.1063/1.5000578>

Submitted: 17 August 2017 . Accepted: 23 October 2017 . Published Online: 08 November 2017

Sergey V. Ryazantsev , Daniil A. Tyurin , Vladimir I. Feldman , and Leonid Khriachtchev 



View Online



Export Citation



CrossMark

ARTICLES YOU MAY BE INTERESTED IN

Communication: A hydrogen-bonded difluorocarbene complex: Ab initio and matrix isolation study

The Journal of Chemical Physics **147**, 131102 (2017); <https://doi.org/10.1063/1.4999772>

Single-reference coupled cluster theory for multi-reference problems

The Journal of Chemical Physics **147**, 184101 (2017); <https://doi.org/10.1063/1.5003128>

Matrix isolation and ab initio study on HCN/CO₂ system and its radiation-induced transformations: Spectroscopic evidence for HCNCO₂ and trans-HCNHCO₂ complexes

The Journal of Chemical Physics **145**, 214309 (2016); <https://doi.org/10.1063/1.4969075>

Lock-in Amplifiers

Find out more today



 Zurich Instruments



Spectroscopic characterization of the complex of vinyl radical and carbon dioxide: Matrix isolation and *ab initio* study

Sergey V. Ryazantsev,^{1,2,a)} Daniil A. Tyurin,¹ Vladimir I. Feldman,¹
 and Leonid Khriachtchev^{2,a)}

¹Department of Chemistry, Lomonosov Moscow State University, 119991 Moscow, Russia

²Department of Chemistry, University of Helsinki, P.O. Box 55, FI-00014 Helsinki, Finland

(Received 17 August 2017; accepted 23 October 2017; published online 8 November 2017)

We report on the preparation and vibrational characterization of the $C_2H_3 \cdots CO_2$ complex, the first example of a stable intermolecular complex involving vinyl radicals. This complex was prepared in Ar and Kr matrices using UV photolysis of propiolic acid (HC_3OOH) and subsequent thermal mobilization of H atoms. This preparation procedure provides vinyl radicals formed exclusively as a complex with CO_2 , without the presence of either CO_2 or C_2H_3 monomers. The absorption bands corresponding to the $\nu_5(C_2H_3)$, $\nu_7(C_2H_3)$, $\nu_8(C_2H_3)$, $\nu_2(CO_2)$, and $\nu_3(CO_2)$ modes of the $C_2H_3 \cdots CO_2$ complex were detected experimentally. The calculations at the UCCSD(T)/L2a level of theory predict two structures of the $C_2H_3 \cdots CO_2$ complex with C_s and C_1 symmetries and interaction energies of -1.92 and -5.19 kJ mol⁻¹. The harmonic vibrational frequencies of these structures were calculated at the same level of theory. The structural assignment of the experimental species is not straightforward because of rather small complexation-induced shifts and matrix-site splitting of the bands (for both complex and monomers). We conclude that the C_1 structure is the most probable candidate for the experimental $C_2H_3 \cdots CO_2$ complex based on the significant splitting of the bending vibration of CO_2 and on the energetic and structural considerations. *Published by AIP Publishing.*
<https://doi.org/10.1063/1.5000578>

I. INTRODUCTION

Vinyl radical (C_2H_3) is a reactive intermediate in combustion processes and chemistry of planetary atmospheres. During the past decades, this species has been extensively characterized by various spectroscopic techniques, both in the gas and solid phases.^{1–14} The experimental studies have provided basic knowledge of the structure and vibrational spectra of vinyl radicals, which is in agreement with the state-of-the-art calculations.^{15–17}

Noncovalent interactions play an important role in many chemical, physical, and biological processes.^{18–20} In particular, the weak interactions of radicals with simple and abundant molecules, such as CO_2 and H_2O , are of great interest for various applications. In general, complexation may affect the reactivity of free radicals. Reactions of vinyl radicals were investigated both experimentally and theoretically (see, e.g., Refs 21 and 22). However, to the best of our knowledge, the intermolecular complexes of this species have not been reported so far. Studies of the complexes of vinyl radicals may be essential for understanding the evolution of this species in real complex systems. The motivation of the present work is to identify a complex between vinyl radicals and carbon dioxide.

Matrix isolation infrared spectroscopy is an efficient tool to study noncovalent interactions.^{23,24} Two related complexes of radicals with CO_2 have recently been characterized by this method. The first example is the $HCNH \cdots CO_2$

complex,²⁵ which is isoelectronic to $C_2H_3 \cdots CO_2$, but has a significantly different molecular structure. The other example is the $C_2H \cdots CO_2$ complex, which exhibits remarkable vibronic interactions due to peculiarities of the electronic properties of the ethynyl radical (C_2H).²⁶

It is not an easy task to produce intermolecular complexes of free radicals in sufficient concentrations in cryogenic matrices. For example, the $HCNH \cdots CO_2$ complexes were obtained by the reactions of H atoms with the $HCN \cdots CO_2$ complexes prepared by deposition of the $HCN/CO_2/Ng$ mixture (Ng = a noble gas).²⁵ In the case of vinyl radicals, the evident way includes the reaction of the $C_2H_2 \cdots CO_2$ complexes with H atoms. Unfortunately, the complex of acetylene with carbon dioxide is quite weak and cannot be obtained in sufficient amounts by co-deposition of C_2H_2 and CO_2 ; thus, one should apply a more sophisticated approach. It has been shown that photolysis of propiolic acid (HC_3OOH , PA) in solid matrices produces the $C_2H_2 \cdots CO_2$ complex with a high yield.²⁷ The reaction of the $C_2H_2 \cdots CO_2$ complexes with H atoms can lead to the $C_2H_3 \cdots CO_2$ complexes. A similar way involving photolysis of a suitable precursor was used to prepare the $HCO \cdots H_2O$ complex.²⁸ In that work, the $HCO \cdots H_2O$ complex was produced by photolysis of $HCOOH/HY/Kr$ (Y = Br and Cl) matrices followed by thermal annealing at about 30 K, which promoted the $H + CO \cdots H_2O \rightarrow HCO \cdots H_2O$ reaction.

In the present work, we report on the experimental and theoretical characterization of the $C_2H_3 \cdots CO_2$ complex. The experimental identification of this complex is performed by using matrix-isolation FTIR spectroscopy. The calculations are done at the UCCSD(T)/L2a level of theory. To the best of

^{a)}Authors to whom correspondence should be addressed: ryazantsev@rad.chem.msu.ru and leonid.khriachtchev@helsinki.fi

our knowledge, it is the first intermolecular complex of vinyl radicals.

II. COMPUTATIONAL AND EXPERIMENTAL DETAILS

A. Computational details

The molecular geometries have been fully optimized (tolerance on gradient: 10^{-6} a.u.) at the valence-correlated UCCSD(T) level of theory.²⁹ The augmented correlation-consistent basis set of type L2a was used.³⁰ This basis set has been successfully used in the previous studies of intermolecular complexes (see, e.g., Ref. 25). The L2a basis set is analogous to the aug-cc-pVTZ basis set,^{31,32} but it includes a larger number of primitive Gaussian functions. The comparison of the basis set contraction schemes for the L2a and aug-cc-pVTZ basis sets is given in Table S1 of the [supplementary material](#). The minimum points on the potential energy surface (PES) were verified by vibrational analysis. Using the optimized geometries, we calculated the harmonic vibrational frequencies, zero-point vibrational energy (ZPVE), and IR intensities at the same level of theory. For the complexes, the interaction energy was found as a difference between energies of the complex and the monomers taking into account the basis set superposition error (BSSE)³³ and ZPVE corrections. Bader's topological analysis of the UCCSD(T)/L2a electron density was performed in order to find the critical points of the electron density (bond critical points (BCPs) and ring critical points).³⁴ All calculations and Bader's topological analysis were performed using the PRIRODA program.³⁵

B. Experimental details

PA ($\geq 98\%$, Alfa Aesar) was degassed by several freeze-pump-thaw cycles. Acetylene (99.6%, AGA), argon ($>99.9999\%$, Linde), and krypton ($>99.999\%$, Linde) were used as purchased. The C_2H_2/Ng and PA/Ng ($Ng = Ar, Kr$) gas mixtures with a typical ratio of 1/2000 were made in a glass bulb by using standard manometric procedures. In the case of PA/Ng mixtures, the bulb was passivated with PA vapors by several fill-keep-evacuate cycles prior to the mixture preparation. The matrices were deposited onto a CsI substrate held at 15 and 20 K for Ar and Kr, respectively, in a closed-cycle helium cryostat (RDK-408D2, SHI). An ArF excimer laser (MSX-250, MPB) provided photolysis at 193 nm (1 Hz, pulse energy density from 5 to 20 $mJ\ cm^{-2}$). An optical parametric oscillator (OPO Sunlite/FX1, Continuum) was used for 250-nm photolysis (10 Hz, pulse energy density $\sim 5\ mJ\ cm^{-2}$). The infrared spectra (region 4000–600 cm^{-1} , resolution 1 cm^{-1} , 500 scans) were measured at 4.3 K with an FTIR spectrometer (Vertex 80, Bruker) equipped with an MCT-B detector. The positions of the infrared absorption bands were obtained from the Gaussian fits, whose standard approximation errors were less than 0.1 cm^{-1} . All experiments were carried out in the University of Helsinki.

III. RESULTS

A. Computational results

The analysis of the PES of the $C_2H_3 \cdots CO_2$ complex gives two structures with C_1 and C_s symmetries corresponding

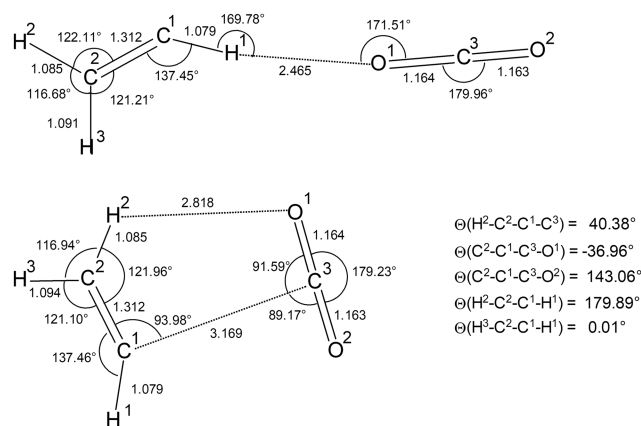


FIG. 1. Structures of the $C_2H_3 \cdots CO_2$ complex with C_s (top) and C_1 (bottom) symmetries. The distances are in Å, and the angles are in degrees. The view on the vinyl radical plane is shown for the C_1 structure (non-planar). Dihedral angles are denoted as Θ . For structures of C_2H_3 and CO_2 monomers, see Fig. S1 of the [supplementary material](#). The atomic coordinates for the $C_2H_3 \cdots CO_2$ complexes and C_2H_3 and CO_2 monomers are given in Table S3 of the [supplementary material](#).

to the true energy minima (Fig. 1). The ZPVE- and BSSE-corrected interaction energies are -5.19 and $-1.92\ kJ\ mol^{-1}$ for the C_1 and C_s complexes. The effect of the corrections is presented in Table S2 of the [supplementary material](#). The structures of the C_2H_3 and CO_2 units in the complex are very similar to those of the monomers (see Fig. S1 of the [supplementary material](#)). The complexation mainly changes the C^2-H^3 and $C^3=O^2$ bond lengths (see Fig. 1 for atom labeling). For both structures, the interaction leads to an elongation of the C^2-H^3 bond and to a shortening of the $C^3=O^2$ bond. For the C_s structure, Bader's topological analysis of the electron density indicates the appearance of one additional BCP between H^1 and O^1 atoms (in comparison with the BCPs of the monomers). For the C_1 structure, a similar analysis shows two additional BCPs corresponding to the $H^2 \cdots O^1$ and $C^1 \cdots C^3$ interactions, which may explain a stronger binding as compared to the C_s structure. The full set of the critical points of the electron density for CO_2 and C_2H_3 monomers and the $C_2H_3 \cdots CO_2$ complex is given in Table S3 of the [supplementary material](#).

The harmonic vibrational frequencies and the IR intensities are presented in Table I. For the $\nu_3(CO_2)$ mode, the calculations predict a red shift of $1.8\ cm^{-1}$ for the C_1 structure and a blue shift of $1.4\ cm^{-1}$ for the C_s structure, as compared to the CO_2 monomer. The complexation results in an increase of the frequency of the $\nu_8(C_2H_3)$ mode: the calculated shift is $+7.0\ cm^{-1}$ for the C_1 structure and $+0.8\ cm^{-1}$ for the C_s structure, as compared to the isolated vinyl radical. The $\nu_2(CO_2)$ vibration is red-shifted by $1.3\ cm^{-1}$ for the C_s structure, and the complexation-induced splitting of this mode is negligible. In the C_1 structure, this mode is split into two components: the stronger one with a considerable red shift ($-9.4\ cm^{-1}$) and the weaker one with a very small red shift ($-0.7\ cm^{-1}$).

B. Experimental results

Monomeric vinyl radicals were prepared by 193-nm irradiation and subsequent annealing of C_2H_2/Ng matrices ($Ng = Ar$ and Kr).⁹ The UV photolysis (1200–3500 pulses, pulse

TABLE I. Calculated vibrational frequencies (in cm^{-1}) for the $\text{C}_2\text{H}_3 \cdots \text{CO}_2$ complex and C_2H_3 and CO_2 monomers.^a

Mode	Monomer ^b	Complex(C_s)	Complex(C_1)
C_2H_3 vibrations			
ν_1 (α -CH str.) ^c	3248.1 (0.5)	3258.8 (12.2)	3249.2 (0.7)
ν_2 (CH_2 a-str.)	3177.5 (2.4)	3173.8 (3.2)	3178.4 (1.0)
ν_3 (CH_2 s-str.)	3070.1 (3.2)	3067.0 (3.9)	3068.4 (2.7)
ν_4 (CC str.)	1636.2 (1.7)	1635.9 (4.0)	1634.6 (2.5)
ν_5 (CH_2 s-bend)	1397.4 (6.7)	1397.5 (5.0)	1397.0 (10.3)
ν_6 (CH_2 a-bend + α -CH bend)	1071.9 (7.1)	1071.6 (10.9)	1071.2 (6.4)
ν_8 (CH_2 + α -CH s-oop bend)	921.9 (69.9)	922.7 (70.4)	928.9 (70.8)
ν_9 (CH_2 + α -CH a-oop bend)	822.3 (9.2)	835.4 (5.0)	818.7 (10.9)
ν_7 (CH_2 + α -CH a-bend)	724.3 (16.8)	731.8 (20.0)	722.7 (16.9)
CO_2 vibrations			
ν_3 (CO_2 a-str.)	2390.0 (649.0)	2391.4 (751.8)	2388.2 (546.9)
ν_1 (CO_2 s-str.)	1346.1 (0.0)	1348.1 (0.1)	1345.8 (0.1)
ν_2 (CO_2 bend)	671.3 (27.2)	670.0 (26.6)	670.6 (22.5)
	671.3 (27.2)	670.0 (26.5)	661.9 (43.4)
Intermolecular vibrations			
		77.4 (2.5)	115.6 (3.5)
		65.2 (0.0)	84.0 (0.2)
		46.7 (1.0)	74.1 (1.2)
		11.6 (0.0)	50.7 (1.2)
		10.8 (0.2)	26.2 (2.1)

^aIR intensities (in km mol^{-1}) are given in parentheses.^bThe data for the C_2H_3 monomer are in agreement with the previous harmonic calculations (see, e.g., Ref. 15).^cAssignment of the vibrational modes of the C_2H_3 radical is according to Ref. 12 (see Ref. 17 for the graphical representation of the normal modes).

energy density $\sim 10 \text{ mJ cm}^{-2}$) partially decomposes matrix-isolated C_2H_2 molecules (by $\sim 30\%$), producing Ng_2H^+ ions (in small amounts), C_2H radicals, and presumably H atoms and C_2 molecules that are invisible in the IR spectra.³⁶ Annealing of Ar and Kr matrices at ~ 20 and 30 K mobilizes H atoms^{37–39} and leads to the formation of vinyl radicals via the $\text{H} + \text{C}_2\text{H}_2 \rightarrow \text{C}_2\text{H}_3$ reaction [trace (a) in Fig. 2].⁹ In addition to the two bands of vinyl radicals previously reported in Ar and Kr matrices (ν_5 and ν_8 modes),⁹ we observed the ν_7 mode ($687.6/684.2 \text{ cm}^{-1}$ in an Ar matrix and $684.7/681.2 \text{ cm}^{-1}$ in a Kr matrix), which is known to be at 677.1 cm^{-1} in a Ne matrix.^{11,13} In a Kr matrix, the $\text{H} + \text{Kr} + \text{CCH}$ reaction leads to the formation of HKrCCH .³⁶

The $\text{C}_2\text{H}_2 \cdots \text{CO}_2$ complexes can be obtained by UV photolysis of PA/Ng matrices.²⁷ In accordance with the previous results,²⁷ 193-nm photolysis (1500 pulses, pulse energy density $\sim 5 \text{ mJ cm}^{-2}$) of matrix-isolated PA leads to the efficient formation of the $\text{C}_2\text{H}_2 \cdots \text{CO}_2$ complex (3302.4 , 3285.3 , 2343.7 , 2340.8 , 1339.5 , 738.2 , 663.6 , and 656.5 cm^{-1} in an Ar matrix and 3292.3 , 3277.9 , 2340.2 , 1330.8 , 734.0 , 661.9 , and 657.1 cm^{-1} in a Kr matrix). Prolonged irradiation (6000 pulses, pulse energy density $15\text{--}20 \text{ mJ cm}^{-2}$) leads to some decrease of the $\text{C}_2\text{H}_2 \cdots \text{CO}_2$ bands. In an Ar matrix, the formation of the $\text{C}_2\text{H} \cdots \text{CO}_2$ complex is observed after extensive photolysis.²⁶ In a Kr matrix, the $\text{C}_2\text{H} \cdots \text{CO}_2$ complex is not detected under these conditions, presumably due to the efficient photodecomposition as discussed elsewhere.²⁶ The $\text{HC}_2\text{OH} \cdots \text{CO}$

and probably $\text{H}_2\text{C}_2\text{O} \cdots \text{CO}$ complexes as well as some other species are also seen after photolysis in small amounts.^{26,27} Prolonged irradiation produces the $\text{HC}_2\text{O} \cdots \text{CO}$ complexes in both matrices (characteristic bands at $2023.8/2019.1 \text{ cm}^{-1}$ in an Ar matrix and at $2020.8/2016.8 \text{ cm}^{-1}$ in a Kr matrix), which evidences the formation of H atoms.

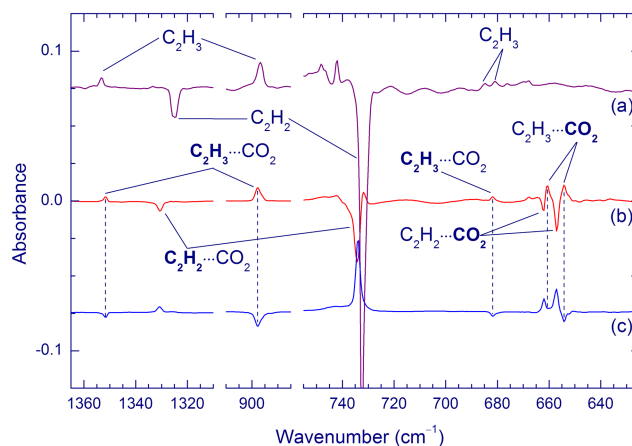


FIG. 2. Difference FTIR spectra showing the results of [(a) and (b)] annealing (5 min at 35 K) of the 193-nm irradiated $\text{C}_2\text{H}_2/\text{Kr}$ and PA/Kr matrices, respectively, and (c) 250-nm irradiation of the preliminary 193-nm irradiated and annealed (5 min at 35 K) PA/Kr matrix. All spectra were measured at 4.3 K.

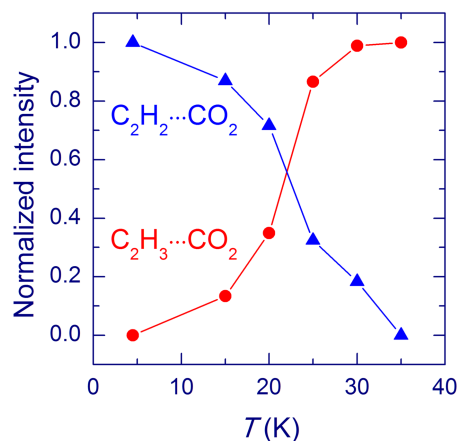


FIG. 3. The effect of annealing (5 min at each temperature) on the formation of the $C_2H_3 \cdots CO_2$ complex and the decrease of the amount of the $C_2H_2 \cdots CO_2$ complex in a Kr matrix. Prior to annealing, a PA/Kr matrix was irradiated at 193 nm. The intensities were obtained by integration of the bands at 897.8 and 734.0 cm^{-1} for $C_2H_3 \cdots CO_2$ and $C_2H_2 \cdots CO_2$, respectively, and normalized to the overall intensity changes. The spectra were measured at 4.3 K.

The UV-irradiated PA/Ng matrices were annealed at 25 and 35 K for Ar and Kr matrices, respectively, which led to some decrease of the amount of $C_2H_2 \cdots CO_2$. Simultaneously, new absorptions appeared in the FTIR spectrum at the positions, which slightly differ from the bands of monomeric C_2H_3 and CO_2 [trace (b) in Fig. 2]. Figure 3 shows that the annealing-induced growth of these new bands is in good correlation with the decrease of the amount of $C_2H_2 \cdots CO_2$. These changes occur in the temperature range, which is characteristic for the thermal mobilization of H atoms.^{37–39} All the bands of the C_2H_3 and CO_2 units are bleached similarly by irradiation at 250 nm, which shows that they originate from the same species. Importantly, the decomposition of $C_2H_3 \cdots CO_2$ at 250 nm is accompanied by an increase of the $C_2H_2 \cdots CO_2$ amount [trace (c) in Fig. 2]. These facts allow us to assign

the new bands to the $C_2H_3 \cdots CO_2$ complex resulting from the reaction of $C_2H_2 \cdots CO_2$ with H atoms. Table II shows the experimental vibrational frequencies of the $C_2H_3 \cdots CO_2$ complex and C_2H_3 and CO_2 monomers. It should be noted that thermally mobilized H atoms in noble-gas matrices cannot react with CO_2 to form HOCO radicals because of large energy barriers for the $H + CO_2 \rightarrow HOCO$ reaction.⁴⁰ Thus, under our experimental conditions, the only possible channel of the reaction between H atoms and $C_2H_2 \cdots CO_2$ is the formation of the $C_2H_3 \cdots CO_2$ complexes. Indeed, no candidates for the $C_2H_2 \cdots HOCO$ complexes in the characteristic regions of the HOCO absorption were observed in our experiments.

IV. CONCLUDING DISCUSSION

In this work, we have reported experimental and theoretical results on the $C_2H_3 \cdots CO_2$ complex, which is the first example of an intermolecular complex of vinyl radicals. The experimental identification of the $C_2H_3 \cdots CO_2$ complex has been performed by using matrix-isolation FTIR spectroscopy. The preparation of this complex in Ar and Kr matrices is based on a two-step synthesis including 193-nm photolysis of PA to yield the precursor complex ($C_2H_2 \cdots CO_2$) followed by its reaction with thermally mobilized H atoms (Figs. 2 and 3). This procedure does not involve isolated C_2H_2 molecules; thus, vinyl radicals are formed exclusively as a complex with CO_2 . In this case, the experimental identification of the complex is straightforward despite rather small spectral shifts induced by the complexation. An interesting direction of further work is to study the effect of complexation on the reactivity of vinyl radicals.

The calculations at the UCCSD(T)/L2a level of theory predict two structures of the $C_2H_3 \cdots CO_2$ complex with C_s and C_1 symmetries (Fig. 1), the latter being lower in energy. Bader's topological analysis of electron density shows two

TABLE II. Experimental vibrational frequencies of C_2H_3 and CO_2 monomers and the $C_2H_3 \cdots CO_2$ complex (complexation-induced shifts in parentheses) and calculated complexation-induced shifts (all values in cm^{-1}).^a

Mode	Ar matrix		Kr matrix		Calculations	
	Monomer	Complex	Monomer	Complex	C_s	C_1
ν_5 (C_2H_3)	1356.7	1357 sh ^b 1354.9 (−1.8)	1353.3	1351.6 (−1.7)	+0.1	−0.4
ν_8 (C_2H_3)	900.4	902.5 (+2.1) ^c 900.0 (−0.4)	896.7	897.8 (+1.1)	+0.8	+7.0
ν_7 (C_2H_3)	687.6 684.7	686.0 (−1.6/+1.3) ^d	684.7 681.2	681.8 (−2.9/+0.6) ^d	+7.5	−1.6
ν_3 (CO_2)	2345.0 2339.4	2342.2 (−2.8/+2.8) ^d	2340.5 2336.6	2339.0 (−1.5/+2.4) ^d	+1.4	−1.8
ν_2 (CO_2)	663.5 662.0	662.5 (−1.0) ^e 653.4 (−10.1) ^e	660.5	661 (+0.5) ^b 654.1 (−6.4)	−1.3 −1.3	−0.7 −9.4

^aExperimental frequencies of the CO_2 monomer are from Ref. 39.

^bTentative assignment.

^cMore intense band of the complex.

^dShifts with respect to each component of the site-split band of the monomer.

^eShifts with respect to the more intense band of the monomer.

additional BCPs for the C_1 structure of the complex corresponding to local atomic interactions between the vinyl radical and carbon dioxide, whereas the C_s structure reveals only one additional BCP. This difference may explain the higher stability of the C_1 structure as compared to the C_s structure. The interaction energy of the C_1 structure of the $C_2H_3 \cdots CO_2$ complex is comparable with that of the most stable (parallel) structure of the $C_2H \cdots CO_2$ complex.²⁶

The structural assignment of the experimental species is not straightforward because of rather small shifts of the observed vibrational bands (Table II). Matrix-site splitting of the experimental bands further complicates the comparison. For the C_2H_3 complex unit, the ν_5 mode is not conclusive, the ν_8 mode is more suitable for the C_s structure, and the ν_7 mode is more suitable for the C_1 structure. For the CO_2 unit, the ν_3 mode is not conclusive, whereas the ν_2 mode features the C_1 structure because of the band splitting and the significant red shift of the stronger component. One should remember that the calculations correspond to the complex in a vacuum, whereas the experiment is performed in a polarizable medium. The matrix effect on the complex structure may be responsible for some inconsistency between experiment and theory. Importantly, the C_1 structure is similar to the structure of the precursor $C_2H_2 \cdots CO_2$ complex produced from PA (parallel geometry),²⁷ so its formation presumably requires a relatively small rearrangement of the complex units and matrix surrounding. Moreover, the C_1 structure is computationally more stable than the C_s structure. There are no clear reasons for a strong structural rearrangement of the system (complex units and matrix) to the less stable C_s structure. Thus, the C_1 structure is the most probable candidate for the experimental $C_2H_3 \cdots CO_2$ complex.

SUPPLEMENTARY MATERIAL

See [supplementary material](#) for the contraction scheme of the L2a basis set, the effects of BSSE and ZPVE corrections on the interaction energies in the $C_2H_3 \cdots CO_2$ complex, and the structure of C_2H_3 and CO_2 monomers. Cartesian atomic coordinates, total energies, and critical points of the electronic density for the $C_2H_3 \cdots CO_2$ complexes and C_2H_3 and CO_2 monomers are also reported.

ACKNOWLEDGMENTS

This work was supported by the Academy of Finland (Project Nos. 1277993 and 1288889) and by the Russian Science Foundation (computational studies, Project No. 14-13-01266). The Joint Supercomputer Center of the Russian Academy of Sciences (Moscow) is gratefully acknowledged for granting computation resources. We also thank Knut Willmann for measuring the reference spectra.

- ¹E. L. Cochran, F. J. Adrian, and V. A. Bowers, *J. Chem. Phys.* **40**, 213 (1964).
- ²P. H. Kasai, *J. Am. Chem. Soc.* **94**, 5950 (1972).
- ³H. E. Hunziker, H. Knepe, A. D. McLean, P. Siegbahn, and H. R. Wendt, *Can. J. Chem.* **61**, 993 (1983).
- ⁴R. A. Shepherd, T. J. Doyle, and W. R. M. Graham, *J. Chem. Phys.* **89**, 2738 (1988).
- ⁵H. Kanamori, Y. Endo, and E. Hirota, *J. Chem. Phys.* **92**, 197 (1990).
- ⁶L. Letendre, D.-K. Liu, C. D. Pibel, J. B. Halpern, and H.-L. Dai, *J. Chem. Phys.* **112**, 9209 (2000).
- ⁷M. B. Pushkarsky, A. M. Mann, J. S. Yeston, and C. B. Moore, *J. Chem. Phys.* **115**, 10738 (2001).
- ⁸K. Tanaka, M. Toshimitsu, K. Harada, and T. Tanaka, *J. Chem. Phys.* **120**, 3604 (2004).
- ⁹H. Tanskanen, L. Khriachtchev, M. Räsänen, V. I. Feldman, F. F. Sukhov, A. Yu. Orlov, and D. A. Tyurin, *J. Chem. Phys.* **123**, 064318 (2005).
- ¹⁰F. Dong, M. Roberts, and D. J. Nesbitt, *J. Chem. Phys.* **128**, 044305 (2008).
- ¹¹Y.-J. Wu, M.-Y. Lin, B.-M. Cheng, H.-F. Chen, and Y.-P. Lee, *J. Chem. Phys.* **128**, 204509 (2008).
- ¹²M. Nikow, M. J. Wilhelm, and H.-L. Dai, *J. Phys. Chem. A* **113**, 8857 (2009).
- ¹³M. E. Jacox and W. E. Thompson, *J. Chem. Phys.* **134**, 064321 (2011).
- ¹⁴P. L. Raston, T. Liang, and G. E. Doublerly, *J. Chem. Phys.* **138**, 174302 (2013).
- ¹⁵A. R. Sharma, B. J. Braams, S. Carter, B. C. Shepler, and J. M. Bowman, *J. Chem. Phys.* **130**, 174301 (2009).
- ¹⁶V. Barone, J. Bloino, and M. Biczysko, *Phys. Chem. Chem. Phys.* **12**, 1092 (2010).
- ¹⁷H.-G. Yu, H. Song, and M. Yang, *J. Chem. Phys.* **146**, 224307 (2017).
- ¹⁸P. Hobza and K. Müller-Dethlefs, *Non-Covalent Interactions: Theory and Experiment* (RSC Publishing, Cambridge, 2010).
- ¹⁹K. E. Riley and P. Hobza, *Wiley Interdiscip. Rev.: Comput. Mol. Sci.* **1**, 3 (2011).
- ²⁰A. S. Mahadevi and G. N. Sastry, *Chem. Rev.* **116**, 2775 (2016).
- ²¹T. L. Nguyen, A. M. Mebel, and R. I. Kaiser, *J. Phys. Chem. A* **105**, 3284 (2001).
- ²²R. Yang, L. Yu, X. Jin, and M. Zhou, *J. Chem. Phys.* **122**, 014511 (2005).
- ²³N. A. Young, *Coord. Chem. Rev.* **257**, 956 (2013).
- ²⁴L. Khriachtchev, *J. Phys. Chem. A* **119**, 2735 (2015).
- ²⁵S. V. Kameneva, D. A. Tyurin, K. B. Nuzhdin, and V. I. Feldman, *J. Chem. Phys.* **145**, 214309 (2016).
- ²⁶S. V. Ryazantsev, R. Tarroni, V. I. Feldman, and L. Khriachtchev, *ChemPhysChem* **18**, 949 (2017).
- ²⁷E. Isoniemi, L. Khriachtchev, M. Makkonen, and M. Räsänen, *J. Phys. Chem. A* **110**, 11479 (2006).
- ²⁸Q. Cao, S. Berski, M. Räsänen, Z. Latajka, and L. Khriachtchev, *J. Phys. Chem. A* **117**, 4385 (2013).
- ²⁹K. Raghavachari, G. W. Trucks, J. A. Pople, and M. Head-Gordon, *Chem. Phys. Lett.* **157**, 479 (1989).
- ³⁰D. N. Laikov, *Chem. Phys. Lett.* **416**, 116 (2005).
- ³¹T. H. Dunning, Jr., *J. Chem. Phys.* **90**, 1007 (1989).
- ³²R. A. Kendall, T. H. Dunning, Jr., and R. J. Harrison, *J. Chem. Phys.* **96**, 6796 (1992).
- ³³S. F. Boys and F. Bernardi, *Mol. Phys.* **19**, 553 (1970).
- ³⁴R. F. W. Bader, *Atoms in Molecules: A Quantum Theory* (Clarendon, Oxford, 1990).
- ³⁵D. N. Laikov and Yu. A. Ustynyuk, *Russ. Chem. Bull.* **54**, 820 (2005).
- ³⁶L. Khriachtchev, H. Tanskanen, A. Cohen, R. B. Gerber, J. Lundell, M. Pettersson, H. Kiljunen, and M. Räsänen, *J. Am. Chem. Soc.* **125**, 6876 (2003).
- ³⁷J. Eberlein and M. Creuzburg, *J. Chem. Phys.* **106**, 2188 (1997).
- ³⁸L. Khriachtchev, M. Saarelainen, M. Pettersson, and M. Räsänen, *J. Chem. Phys.* **118**, 6403 (2003).
- ³⁹S. V. Ryazantsev and V. I. Feldman, *J. Phys. Chem. A* **119**, 2578 (2015).
- ⁴⁰J. Li, C. Xie, J. Ma, Y. Wang, R. Dawes, D. Xie, J. M. Bowman, and H. Guo, *J. Phys. Chem. A* **116**, 5057 (2012).